Fischer, Michael

Water adsorption in SAPO-34: Elucidating the role of local heterogeneities and defects using dispersion-corrected DFT calculations

Journal Article	as:	peer-reviewed accepted version (Postprint)
DOI of this document*(secondary publication):		https://doi.org/10.26092/elib/2856
Publication date of this document:		11/03/2024

* for better findability or for reliable citation

Recommended Citation (primary publication/Version of Record) incl. DOI:

Water adsorption in SAPO-34: Elucidating the role of local heterogeneities and defects using dispersion-corrected DFT calculations, reproduced from: M. Fischer, Phys. Chem. Chem. Phys. 2015, 17, 25260-25271. http://doi.org/10.1039/c5cp04189a

Water adsorption in SAPO-34: elucidating the role of local heterogeneities and defects using dispersion-corrected DFT calculations†

Michael Fischer

The chabazite-type silicoaluminophosphate SAPO-34 is a promising adsorbent for applications in thermal energy storage using water adsorption–desorption cycles. In order to develop a microscopic understanding of the impact of local heterogeneities and defects on the water adsorption properties, the interaction of different models of SAPO-34 with water was studied using dispersion-corrected density-functional theory (DFT-D) calculations. In addition to SAPO-34 with isolated silicon atoms, the calculations considered models incorporating two types of heterogeneities (silicon islands, aluminosilicate domains), and two defect-containing (partially and fully desilicated) systems. DFT-D optimisations were performed for systems with small amounts of adsorbed water, in which all H_2O molecules can interact with framework protons, and systems with large amounts of adsorbed water (30 H_2O molecules per unit cell). At low loadings, the host–guest interaction energy calculated for SAPO-34 with isolated Si atoms amounts to approximately -90 kJ mol^{-1}. While the presence of local heterogeneities leads to the creation of some adsorption sites that are energetically slightly more favourable, the interaction strength is drastically reduced in systems with defects. At high water loadings, energies in the range of -70 kJ mol^{-1} are obtained for all models. The DFT-D interaction energies are in good agreement with experimentally measured heats of water adsorption. A detailed analysis of the equilibrium structures was used to gain insights into the binding modes at low coverages, and to assess the extent of framework deprotonation and changes in the coordination environment of aluminium atoms at high water loadings.

Introduction

Aluminophosphates (AlPOs) and silicoaluminophosphates (SAPOs) have attracted considerable interest as potential adsorbent materials for heat storage and heat transformation applications that use water as working fluid.[1–4] SAPOs/AlPOs exhibit water uptakes and energy densities similar to those of typical aluminosilicate zeolites, however, they have been deemed to be more suitable for heat storage at moderate temperatures by virtue of their lower desorption temperatures: as complete desorption of water can be reached in a range between 95 and 140 °C, only moderate driving heats would be needed in the regeneration phase of the adsorption cycle.[4,5] Among these materials, SAPO-34, which has chabazite topology, has been identified as a particularly promising adsorbent.[2–8] Significant steps towards application have been made, *e.g.* through the preparation of SAPO-34 coatings on aluminium for use in heat exchangers.[7,8]

Fachgebiet Kristallographie, Fachbereich Geowissenschaften, Universität Bremen, Klagenfurter Straße 2, 28359 Bremen, Germany. E-mail: michael.fischer@uni-bremen.de

† Electronic supplementary information (ESI) available: DFT-D energies of snapshots, visualisation of selected systems, typical CASTEP input files. See DOI: 10.1039/c5cp04189a

Due to the importance of SAPO-34 as catalyst for methanol-to-olefin conversions, there are a number of publications investigating the structure and stability of this system with a portfolio of experimental and theoretical methods. While a comprehensive overview cannot be given in this context, some findings of particular relevance will be summarised. The first point concerns the incorporation of silicon atoms in the framework: on the one hand, silicon atoms can replace phosphorus at isolated T sites of an AlPO-34 matrix. These isolated Si atoms are surrounded by Si–O–Al linkages, and a proton is bonded to one of the neighbouring oxygen atoms to balance the charge. On the other hand, ''silicon islands'' can form, *e.g.* by substituting one Al and four P atoms with five Si atoms (substitution patterns that lead to Si–O–P linkages were found to be unstable[9]). When such silicon islands are formed, less than one proton per framework silicon atom is necessary to balance the charge (*e.g.* three protons for a 5-atom silicon island). As an intermediate scenario between isolated Si atoms and silicon islands, local aluminosilicate domains in which only aluminium and silicon atoms alternate on the T sites could also occur.[10] Recent computations have delivered evidence for the stability of such ''next-nearest-neighbour'' arrangements.[11]

A peculiar feature of SAPO-34 is the dependence of the water adsorption properties on the sample preparation route: as shown by Henninger and co-workers, SAPO-34 synthesised with morpholine as template molecule exhibits a rapid loss of the water adsorption capacity in water adsorption–desorption cycles, whereas SAPO-34 samples synthesised with other templates are much more stable, with only negligible loss of capacity over approximately 30 cycles.[2,3] This observation can be directly linked to the previous finding that the distribution of silicon in the framework can be influenced by the choice of the template molecule: for SAPO-34 with a moderate silicon content (~10% of the T atoms are silicon), the morpholine route favours isolated Si atoms, whereas use of a tetraethylammonium hydroxide template leads to the formation of silicon islands.[10] A post-synthesis heat treatment was found to decrease the number of isolated Si atoms, and to increase the number of Si–O–Si linkages, a phenomenon that was ascribed to a concurrent desilication and dehydroxylation of the framework, followed by the migration of silicon atoms to form silicon islands.[12] With increasing silicon content, a larger fraction of the Si atoms are incorporated in silicon islands.[10,13] A computational study using empirical potential models, which compared SAPO-34 and SAPO-5, showed that the relative stability of silicon islands depends on the framework topology.[14] Furthermore, it was deduced from the calculations that protons in the vicinity of silicon islands have a higher acidity than those near isolated Si atoms, a finding that was substantiated in subsequent experimental and theoretical studies.[15,16] Computational methods were also employed to predict the most stable proton arrangement around a 5-atom silicon island,[17] and the most stable configuration of pairs of protons associated with two isolated Si atoms.[11]

Upon water adsorption, all adsorbed H_2O molecules can directly interact with the framework protons at low water loadings (up to one water molecule per proton).[18,19] At higher water loadings (approaching saturation), the interaction with framework Al atoms can induce structural transformations. In an early diffraction study, Minchev *et al.* observed a significant loss of crystallinity of SAPO-34 upon water adsorption.[20] However, dehydration restored the crystallinity. It was shown subsequently that the crystallinity of a SAPO-34 sample containing silicon islands can be restored after a prolonged exposure to humidity, whereas samples with isolated Si atoms lose their crystallinity irreversibly.[21] This was explained with the increased likelihood of a hydrolysis of Si–O–Al linkages in systems that contain mostly isolated Si atoms. As shown by means of MAS NMR experiments, the adsorption of H_2O molecules at the framework protons is followed by the coordination of water to framework aluminium atoms, leading to the formation of octahedrally coordinated Al atoms.[19] While this process is fully reversible at room temperature, steaming at elevated temperatures may lead to the removal of silicon atoms from the framework. The desilication and subsequent redistribution of silicon atoms has been studied in detail in a series of computational studies employing density-functional theory (DFT).[22–24]

Another question related to the adsorption of water molecules is whether the adsorbed water molecules interact with framework protons exclusively through hydrogen bonds, or whether they can deprotonate the framework to form hydronium ions. Based on early IR spectroscopy experiments, it was postulated that a stoichiometric formation of hydronium ions occurs at room temperature.[25] A combined neutron diffraction and IR study of water-loaded SAPO-34 pointed to the simultaneous presence of hydrogen-bonded water molecules and hydronium ions.[26] According to more recent spectroscopic investigations, however, only a limited amount of protonated water clusters form in SAPO-34 at high water loadings, whereas a large fraction of the available protons remain attached to the framework oxygen atoms.[18] Computational studies corroborated that the protonation of water molecules becomes more likely when the amount of water increases: in an early *ab initio* Molecular Dynamics (MD) study, no indications for the formation of isolated hydronium ions were found, but it was predicted that $(H_2O)\cdot(H_3O)^+$ clusters may form when two water molecules are adsorbed near one framework proton.[27] According to later computational works dealing with aluminosilicate zeolites, an even larger number of water molecules per acid site may be necessary to stabilise protonated clusters, especially when temperature effects are taken into account.[28,29]

On a qualitative level, it has been established that variations in the local structure of SAPO-34 like silicon islands and structural defects affect the water adsorption properties. However, a quantitative atomistic description based on computational chemistry methods has not yet been attempted. In this study, dispersion-corrected DFT calculations were employed to study the interaction of various models of SAPO-34 with adsorbed water molecules. The following models were considered:

- SAPO-34 with isolated silicon atoms
- SAPO-34 with a 5-atom silicon island
- Partially and fully desilicated SAPO-34, containing defects in place of some/all framework silicon atoms
- Pure (defect-free) aluminophosphate AlPO-34

The inclusion of desilicated models was motivated by the earlier, detailed computational studies of SAPO-34 desilication by Fjermestad *et al.*, who showed that the removal of silicon atoms from the framework can occur in the presence of water through hydrolysis of Si–O–Al linkages.[22–24] The interaction of the different systems with adsorbed water at low and high water loadings was predicted from the calculations, and the optimised structures were analysed to identify binding modes and structural changes upon water adsorption. While the chosen approach delivers only a "static" picture, and cannot capture phenomena like progressive structural decomposition upon interaction with water, the present study enhances our understanding of how local heterogeneities and defects in SAPO-34 affect the water adsorption properties. It can thus aid the atomic-level interpretation of experimental findings.

Computational details and models of SAPO-34

DFT calculations

Dispersion-corrected DFT (DFT-D) calculations were performed using the CASTEP code, which uses a combination of plane

waves and pseudopotentials.[30] The calculations used on-the-fly generated ultrasoft pseudopotentials and an energy cutoff of 700 eV. Due to the size of the hexagonal unit cell of SAPO-34, only the gamma point was used to sample the Brillouin zone. The calculations employed the PBE exchange–correlation functional[31] in conjunction with the dispersion correction proposed by Tkatchenko and Scheffler (TS).[32] In a previous study that investigated the performance of several exchange–correlation functionals in reproducing the properties of different phases of ice, the PBE-TS functional delivered only moderately good agreement with experiment, exhibiting a systematic overestimation of lattice energies.[33] However, it does give a molecular dispersion coefficient C_6 of water that agrees very well with the experimental value. The PBE-TS functional has been successfully employed for the structure optimisation of sheet silicates, where it outperforms a variety of other functionals with and without dispersion corrections,[34] and in a study of water/glycine coadsorption on copper surfaces.[35] Our own benchmarking investigation showed that the structures of water-containing zeolites predicted with this functional are mostly in very good agreement with experimental data.[36]

The interaction energies reported throughout this paper were obtained from the following equation:

$$E_{int} = E_{PBE\text{-}TS}(\text{SAPO-34} + nH_2O) - E_{PBE\text{-}TS}(\text{SAPO-34}) - nE_{PBE\text{-}TS}(H_2O)$$

The first term on the right hand side of the equation corresponds to the PBE-TS energy for a model of SAPO-34 with n adsorbed water molecules, the second term represents the guest-free system, and the last term corresponds to the energy obtained for a single water molecule in a box with an edge length of 20 Å, multiplied by n. In order to strictly compare the DFT-D results to experimental heats of adsorption, it would be necessary to include the zero-point vibrational energy, as well as temperature contributions. However, due to the computational overhead of the additional calculations, it was not attempted to compute these quantities. In a previous study of water adsorbed in aluminosilicate chabazite, a ZPVE correction of approximately +5 to +10 kJ mol^{-1} was obtained from PBE calculations.[29] Temperature contributions can be approximated by including an RT term, which would amount to −2.5 kJ mol^{-1} for a temperature of 300 K. It can thus be estimated that the heats of adsorption measured at room temperature should be approximately 5 (±2.5) kJ mol^{-1} lower than the DFT-D interaction energies (in absolute terms: while E_{int} is negative, the heat of adsorption is positive by definition).

Models of guest-free SAPO-34 systems

Models of SAPO-34 incorporating different distributions of the silicon atoms, as well as structural defects, were constructed and optimised with DFT-D calculations. In all cases, the structure optimisation included a relaxation of the lattice parameters. To start with, the structure of the aluminophosphate AlPO-34 was taken from the literature.[37] A model of SAPO-34 with isolated silicon atoms was constructed from AlPO-34 as follows: in each double six-ring unit (d6R), one phosphorus atom was replaced with silicon, thereby reducing the symmetry from $R\bar{3}$ to $P3_2$.

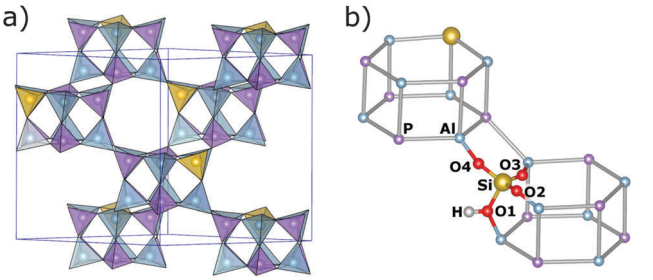

Fig. 1 (a) Representation of the structure of SAPO-34 with isolated Si atoms as tetrahedral framework. SiO_4 tetrahedra are shown in yellow, AlO_4 tetrahedra in cyan, and PO_4 tetrahedra in light purple. (b) Enumeration of oxygen atoms employed in this work, taking SAPO-34_O1 as example. The environment of one isolated silicon atom is shown in an atomistic representation, whereas the remainder of the d6R units is displayed schematically. All structure figures were prepared using VESTA 3.0.[57]

Thus, silicon atoms occupy one twelfth of the available T sites, an amount that is typical for relatively silicon-poor samples of SAPO-34 that can be synthesised with different template molecules.[10] For the calculations, four separate models were prepared, in which the framework proton that balances the charge was attached to different oxygen atoms surrounding the silicon atom. It is worth noting that different ways to enumerate the oxygen atoms in chabazite-type structures have been used by different researchers.[26,38–41] In the following, we use the enumeration employed by Smith and co-workers, which is displayed in Fig. 1.[26,40,41] The systems are labelled according to the position of the framework proton: for example, the proton is bonded to the oxygen atom O1 in SAPO-34_O1.

The model of SAPO-34 with a silicon island (termed SAPO-34_Si_island throughout this work) is based on earlier work by Zokaie *et al.*[17] Using a combination of molecular mechanics and DFT calculations, these authors assessed the stability of a total of 108 possible proton distributions around a five-atom silicon island (the smallest possible silicon island that does not include unstable Si–O–P linkages), and derived criteria to predict unstable distributions. In the most stable arrangement found in their work, shown in Fig. 2a, two protons are bonded to O1 atoms, and the third proton is bonded to an O3 atom. It is worth noting that this system contains a larger number of silicon atoms per unit cell than SAPO-34 with isolated silicon atoms (five instead of three), but that the number of framework protons is the same. In order to generate a model with a local "aluminosilicate" domain (SAPO-34_SiAl_domain), the central Si atom of SAPO-34_Si_island was replaced by an Al atom, and an additional proton was added at the O1 atom neighbouring this Al atom to balance the charge (Fig. 2b).

The first model of SAPO-34 incorporating a silicon defect (SAPO-34_defect + $Si(OH)_4$) was constructed along the lines of the previous computational study of Fjermestad *et al.*, who investigated the dealumination of SSZ-13, and the desilication of SAPO-34.[22] In their final desilicated structure of SAPO-34, the silicon atom has left the framework, forming an extra-framework $Si(OH)_4$ molecule (orthosilicic acid). The aluminium atoms that were originally neighbouring the silicon atom are now saturated

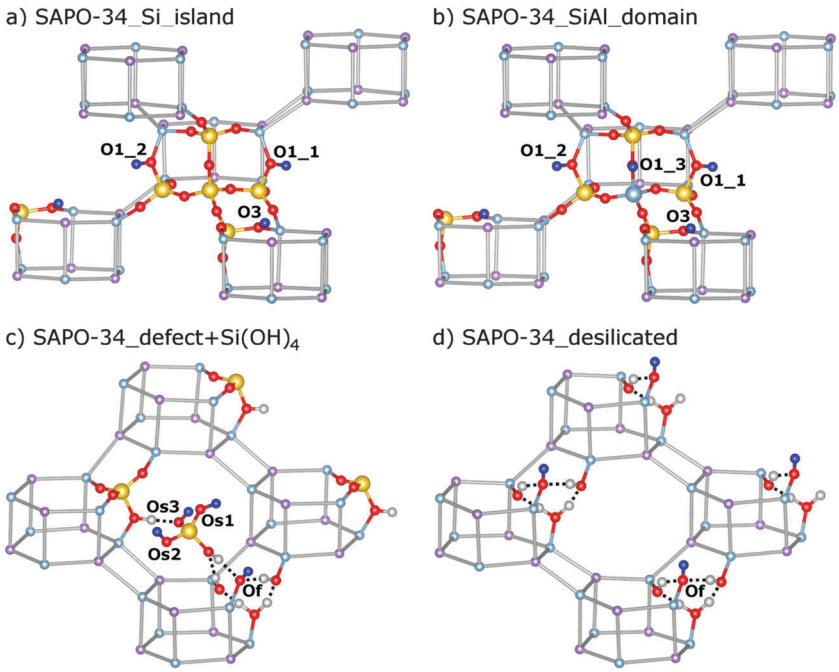

Fig. 2 Visualisation of models of SAPO-34 that incorporate local heterogeneities or defects. Like in Fig. 1b, Al–O–P linkages are only shown schematically. Protons that are not involved in hydrogen bonds, and thus accessible to adsorbed water molecules, are highlighted in blue. Labels refer to the oxygen atoms to which the protons are bonded.

by three hydroxyl groups and one aqua ligand. Because a network of hydrogen bonds forms between neighbouring hydroxyl groups, only four of the nine protons associated with the defect and the $Si(OH)_4$ molecule are accessible to guest molecules. These protons are labelled explicitly in Fig. 2c, with Os representing protons of the $Si(OH)_4$ group, and Of being a proton attached to a framework oxygen atom. In the original structure from the previous work of Fjermestad *et al.*, there is one defect per d6R unit, while the structure used in the current work contains one defect and two intact d6R units per (hexagonal) unit cell. The construction of a fully desilicated model of SAPO-34 (SAPO-34_desilicated) was also based on the work of Fjermestad *et al.*[22] In this case, their final desilicated structure, in which all silicon atoms have left their positions in the framework, was modified by removing the orthosilicic acid groups. Of the five protons associated with the defect (three hydroxyl groups and one aqua ligand), only one does not participate in hydrogen bonds, as shown in Fig. 2d. This corresponds to a scenario in which the $Si(OH)_4$ units have been able to diffuse out of the structure, and in which the defects caused through silicon removal are not "healed" through the migration of phosphorus onto the vacant T sites.[24] While this model includes a number of *a priori* assumptions regarding the nature of the defect, it should be a reasonably realistic representation of a heavily defective SAPO-34 system.

Models of SAPO-34 with adsorbed water molecules

The interaction of SAPO-34 with water at low water loadings was studied by adding one or a few H_2O molecules to the structure: in cases where several framework protons in the unit cell have the same environment (SAPO-34 with isolated Si atoms and SAPO-34_desilicated), one water molecule per d6R unit was added, *i.e.* the full unit cell contains three water molecules (macroscopically, this corresponds to a loading of roughly 21 g H_2O per kg adsorbent). In those systems where all hydrogen atoms in the unit cell have a different environment (SAPO-34_Si_island, SAPO-34_SiAl_domain, SAPO-34_defect + $Si(OH)_4$), separate structures with one water molecule per cell were constructed for each framework proton. In each case, the water molecules were placed in the close proximity of a framework proton. In a previous computational study, a number of local minima were found for a water molecule adsorbed at a given proton site of SAPO-34.[27] As these minima are rather close in energy, the sampling in the present work is restricted to one local minimum per framework proton. The same strategy was employed in many previous computational works dealing with the adsorption of polar guests at the framework protons of SAPO-34.[16,17,29,42]

To generate initial configurations of a larger number of water molecules in the pores of SAPO-34, Monte Carlo simulations were performed for all adsorbent systems considered. These calculations used the Sorption module included in the Accelrys Materials Studio suite. The simulations were performed for a loading of 30 water molecules per unit cell. This corresponds to roughly 210 g kg^{-1}, a water loading that is typically attained at moderate relative pressures.[4,6] The simulations used Lennard-Jones parameters and charges from the Consistent Valence Force field (CVFF) for the water molecules and framework atoms.[43] While further validation would be necessary when aiming at quantitative predictions, these parameters should be sufficiently accurate to generate realistic starting configurations for the subsequent DFT-D calculations. For each adsorbent, a simulation run

comprising five million production steps was performed. A total of five snapshots from different stages of the simulation were chosen randomly, and optimised using the DFT-D approach outlined above. It has to be considered that the DFT-D optimisation of a snapshot will not deliver the global energy minimum, but a local minimum. In this complex system, a near-infinite number of local minima coexist, which are close in energy. In a real adsorption experiment, many of these minima will be sampled. In order to calculate an approximate value of the interaction strength, a simple averaging over the DFT-D interaction energies obtained for the five optimised snapshots can be performed. While this is a rather simplistic approach, it should give a realistic estimate of the average interaction energy. For a more comprehensive sampling, *ab initio* MD simulations starting from different initial configurations should be performed, but these are beyond the scope of the present study.

In the DFT-D calculations for SAPO-34 models with adsorbed water molecules, the lattice parameters were fixed to the values obtained for the guest-free systems, after establishing in preliminary calculations that the lattice distortions upon adsorption of 30 water molecules per cell remain modest (relative changes of less than 1% in the lattice parameters).

Results and discussion

DFT-D optimisation of guest-free SAPO-34 models

The four structures of SAPO-34 with isolated silicon atoms were optimised using DFT-D calculations. A comparison of the total energies showed that SAPO-34_O1 is the energetically most favourable situation, with SAPO-34_O3 being 2.3 kJ mol^{-1} (per framework proton) less favourable, and the other two possibilities approximately 9 kJ mol^{-1} less favourable. Due to the small energy differences, it can be expected that the protons are most likely found at O1, but that they may also occupy other sites with a certain probability at finite temperature, as discussed in an earlier DFT study.[44] The energetic order is in partial agreement with a neutron diffraction study of hydrated SAPO-34, where framework protons attached to O1 and O2 were observed.[26] The same proton sites were found in a neutron diffraction study of H-SSZ-13 (an aluminosilicate with chabazite topology),[41] whereas protons bonded to O2 and O4 were observed in a neutron diffraction study of dehydrated SAPO-34.[40] Previous DFT studies also delivered O1 as the energetically preferred proton site in SAPO-34 and related chabazite-type materials.[39,45] Throughout this article, protons bonded to a certain framework atom OX are designated as H–OX for brevity.

The DFT-D optimised lattice parameters of the four systems, listed in Table 1, fall in a relatively narrow range, with a ranging between 13.80 and 13.89 Å and c varying from 14.89 to 15.15 Å (due to the trigonal symmetry of these systems, there are no deviations from the hexagonal cell metric). These values are in very good agreement with the lattice parameters reported in a neutron diffraction study of fully dehydrated SAPO-34 (a = 13.774 Å, c = 15.016 Å), with the maximal absolute (relative) deviations remaining below 0.15 Å (1%).[40]

Table 1 DFT-D optimised lattice parameters for all structures considered

	a/Å	b/Å	c/Å	α/deg	β/deg	γ/deg
SAPO-34_O1	13.805	13.805	15.149	90	90	120
SAPO-34_O2	13.851	13.851	15.012	90	90	120
SAPO-34_O3	13.856	13.856	15.012	90	90	120
SAPO-34_O4	13.886	13.886	14.894	90	90	120
SAPO-34_Si_island	13.840	13.855	15.088	89.92	89.96	120.36
SAPO-34_SiAl_domain	13.845	13.858	15.131	90.01	89.95	120.23
SAPO-34_defect + $Si(OH)_4$	13.833	13.754	14.893	88.93	89.92	119.63
SAPO-34_desilicated	14.188	14.055	14.243	86.76	89.41	122.61
AlPO-34	13.792	13.792	14.981	90	90	120

The DFT-D optimisation of the SAPO-34_Si_island model delivered lattice parameters that are very similar to those obtained for SAPO-34 with isolated silicon atoms, with only minimal deviations from the hexagonal cell metric (Table 1). The same applies for the SAPO-34_SiAl_domain model. In the first of the defect-containing models, SAPO-34_defect + $Si(OH)_4$, the lattice parameters b and c are slightly shorter than in the defect-free systems, but the angles remain close to the hexagonal values. In the second system, SAPO-34_desilicated, the optimised unit cell parameters are significantly different from those of the other SAPO-34 models: the c-axis is about 0.8 Å shorter, and a- and b-axes are roughly 0.2 to 0.3 Å longer. Furthermore, the angles deviate from the hexagonal metric by up to three degrees. Finally, the optimisation of the pure aluminophosphate AlPO-34 delivered lattice parameters in excellent agreement with the experimentally determined values for the template-free system, which were reported by Amri and Walton (a = 13.744 Å, c = 14.941 Å at T = 110 K).[37]

Spectroscopic signature of framework protons: semi-quantitative interpretation

IR spectroscopic experiments on guest-free SAPO-34 have revealed the presence of at least two distinct bands in the frequency range of the O–H stretching mode ν(OH): a high-frequency band at approximately 3630 cm^{-1} and a low-frequency band at approximately 3600 cm^{-1}.[15,18,40] These two bands were ascribed to vibrations associated with protons bonded to different framework oxygen atoms, whereas a third feature observed at 3617 cm^{-1} was explained as being due to protons near the border of silicon islands.[15] In previous computational studies, it was found that the calculated frequency does indeed depend on the oxygen atom to which the proton is bonded, however, there was a systematic tendency to underestimate the difference between the ν(OH) values associated with the high-frequency and the low-frequency modes.[45,46] While the present study does not aim at a direct prediction of the IR stretching frequencies, some semi-quantitative conclusions can be drawn by making use of the ν(OH)–d(O–H) correlation developed by Nachtigall and co-workers. This correlation permits the calculation of the ν(OH) value from the bond length d(O–H) calculated with the PBE functional. When it is assumed that the inclusion of the TS dispersion correction has no significant influence on the bond length, the previously published parameters for this correlation, obtained using the PBE functional (see Table 1 of ref. 47), can be employed to calculate ν(OH). In order to test the validity

Table 2 DFT-D optimised oxygen-hydrogen bond lengths d(O–H) and associated stretching frequencies ν(OH) calculated using the ν(OH)–d(O–H) correlation developed by Nachtigall and co-workers.[47] Systems with frequencies exceeding 3650 cm^{-1} (high-frequency band, see text) are highlighted in italics[a]

SAPO-34_X, X = ...	d(O–H)/Å	ν(OH)/cm^{-1}
O1	*0.9735*	*3656*
O2	0.9753	3632
O3	0.9754	3631
O4	0.9756	3628
Si_island, H–O1_1	*0.9737*	*3653*
Si_island, H–O1_2	*0.9737*	*3653*
Si_island, H–O3	0.9758	3625
SiAl_domain, H–O1_1	*0.9729*	*3663*
SiAl_domain, H–O1_2	*0.9728*	*3665*
SiAl_domain, H–O1_3	*0.9724*	*3670*
SiAl_domain, H–O3	0.9757	3626

[a] As discussed in more detail in the text, the PBE functional used in ref. 47 and the PBE-TS functional employed here give O–H distances that vary by up to 5×10^{-4} Å, leading to an approximate uncertainty of 7 cm^{-1} in the calculated frequencies.

of this assumption, the d(O–H) values of the PBE-TS structures were compared to the analogous bond distances obtained in separate optimisations using the PBE functional without dispersion corrections. The observed differences did not exceed 5×10^{-4} Å, corresponding to a difference of not more than 7 cm^{-1} in the respective frequencies. As this is clearly sufficient for the desired semi-quantitative interpretation, the parameters of the ν(OH)–d(O–H) correlation published in ref. 47 are applicable in the context of the present work.

Table 2 lists the bond lengths d(O–H) obtained for the SAPO-34_OX, SAPO-34_Si_island, and SAPO-34_SiAl_domain systems, as well as the ν(OH) values calculated using the ν(OH)–d(O–H) correlation. Like the experimental spectra, the calculated frequency values can be divided into two groups: frequencies ranging from 3625 to 3632 cm^{-1} are associated with H–O2, H–O3, and H–O4 protons, whereas frequencies between 3653 and 3670 cm^{-1} are calculated for protons bonded to O1 atoms. In the latter group, frequency values around 3655 cm^{-1} are obtained for SAPO-34_O1 and SAPO-34_Si_island, whereas significantly higher frequencies in the range of 3665 cm^{-1} are obtained for the H–O1 protons in the system containing an aluminosilicate domain. Compared to the experimentally measured bands, there is a shift of at least 25 cm^{-1} towards higher wavenumbers, which is not surprising given the approximations made. For SAPO-34_OX and SAPO-34_Si_island, the difference between the low-frequency and high-frequency band of roughly 30 cm^{-1} is reproduced very well by the calculations; however, the prediction of even higher frequency values for SAPO-34_SiAl_domain does not correlate with any experimental observation. Two main conclusions can be drawn at this point: firstly, the calculations indicate that the high-frequency band can be ascribed to H–O1 protons, whereas the low-frequency band is due to protons associated with other framework oxygens. This differs from previously proposed interpretations of experimental spectra, where the high-frequency band was attributed either to H–O4 protons,[40] or to protons bonded to any framework oxygen except O2.[15,18] Secondly, the calculations for the systems with a small (5-atom) silicon island and aluminosilicate domain deliver no explanation for the additional band at 3617 cm^{-1} observed experimentally. Computations using appropriate supercells could help to elucidate whether this band can be assigned to protons associated with larger silicon islands or more extended aluminosilicate domains, as proposed in a previous spectroscopic investigation.[15]

Interaction of defect-free SAPO-34 with adsorbed water molecules

This section presents the DFT-D results obtained for defect-free models of SAPO-34 (SAPO-34_OX, SAPO-34_Si_island, SAPO-34_SiAl_domain) with adsorbed water. For low water loadings (1 or 3 H_2O molecules per unit cell), the resulting interaction energies E_{int} as well as selected interatomic distances are given in Table 3.

In SAPO-34 with isolated silicon atoms, the energies obtained for systems in which the proton is bonded to different oxygen atoms fall in a rather narrow range (−89.9 to −92.8 kJ mol^{-1}), *i.e.* the framework–H_2O interaction at low water loadings is practically independent of the proton position. As pointed out above, the DFT-D interaction energy is not equivalent to the experimentally accessible heat of adsorption. Nevertheless, it is insightful to compare the two quantities. From adsorption measurements, Jänchen and Stach calculated a heat of adsorption of approximately 85 kJ mol^{-1} at low water coverages, where all water molecules can interact with framework protons.[6] Bearing in mind the systematic difference between DFT-D interaction energies and heat of adsorption, which, as discussed above, is expected to amount to 5 (±2.5) kJ mol^{-1}, the agreement between the two quantities is very good. This indicates that the chosen computational approach allows for a relatively accurate prediction of the interaction strength.

Regarding the structures of the adsorption complexes, two different cases can be distinguished: for SAPO-34_O1, _O2, and _O4, there is only one short hydrogen bond, which is formed between the framework proton and the oxygen atom of the water molecule ($d(H\cdots O_{H_2O}) \approx 1.53$ Å). The secondary contacts between the hydrogen atoms of the water molecule and framework oxygen atoms are significantly longer ($d(H_{H_2O}\cdots O) > 2$ Å). Their length varies considerably among the different systems, depending on the local environment. The equilibrium structure of H_2O@SAPO-34_O1 is shown in Fig. 3a. In contrast to this, the water molecule assumes a tripod-like configuration above the d6R unit in SAPO-34_O3, with three relatively short hydrogen bonds (all below 2 Å, see Fig. 3b). Due to the presence of an additional hydrogen bond, the non-dispersive contribution to the total interaction is somewhat larger than for the other three SAPO-34_OX systems, but the total interaction energy remains in the same range. Furthermore, the bond between the proton and the framework oxygen atom is elongated more strongly in this system: compared to the guest-free system, d(O–H) is elongated by approximately 0.10 Å in SAPO-34_O3, whereas the elongation Δd(O–H) amounts to approximately 0.06 Å in the other systems. In summary, we observe a distinct binding mode in SAPO-34_O3,

Table 3 DFT-D results obtained for small amounts of water adsorbed in defect-free models of SAPO-34. The table includes the interaction energy per H_2O molecule (E_{int}), the non-dispersive contribution to the total interaction energy ($E_{int,nodisp}$) in absolute and relative terms (in per cent, values in brackets), as well as relevant interatomic distances (see text)

SAPO_34_X, X = ...	E_{int}/kJ mol^{-1}	$E_{int,nodisp}$/kJ mol^{-1} (%)	d(H···O_{H_2O})/Å	d(H_{H_2O}···O)/Å	d(O–H)/Å	Δd(O–H)/Å
O1, H_2O@H–O1	−92.8	−71.7 (77)	1.536	2.17; 2.84	1.033	0.059
O2, H_2O@H–O2	−92.3	−71.3 (77)	1.528	2.08; 2.85	1.040	0.064
O3, H_2O@H–O3	−90.9	−72.6 (80)	1.411	1.90; 1.91	1.079	0.104
O4, H_2O@H–O4	−89.9	−69.5 (77)	1.530	2.66; 2.71	1.041	0.065
Si_island, H_2O@H–O1_1	−95.0	−73.8 (78)	1.523	2.34; 2.51	1.035	0.061
Si_island, H_2O@H–O1_2	−95.5	−74.2 (78)	1.519	2.36; 2.42	1.037	0.063
Si_island, H_2O@H–O3	−93.3	−75.0 (80)	1.388	1.86; 1.89	1.090	0.114
SiAl_domain, H_2O@H–O1_1	−91.6	−71.0 (78)	1.535	2.03; 2.86	1.031	0.058
SiAl_domain, H_2O@H–O1_2	−94.0	−72.9 (78)	1.539	2.10; 2.88	1.031	0.059
SiAl_domain, H_2O@H–O1_3	−99.1	−78.6 (79)	1.528	1.92; 2.89	1.035	0.062
SiAl_domain, H_2O@H–O3	−86.2	−69.0 (80)	1.446	1.90; 1.92	1.063	0.087

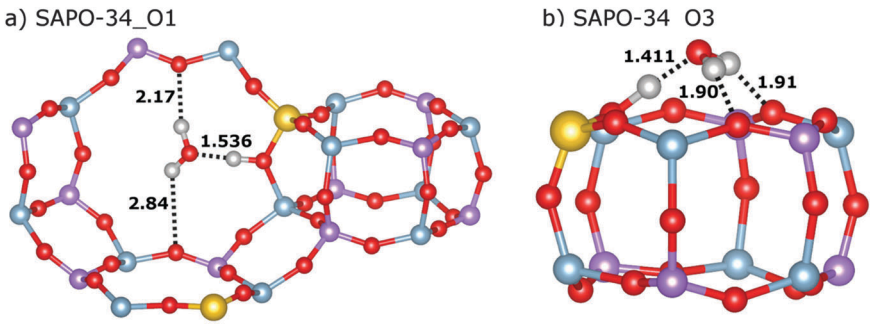

Fig. 3 Environment of the water molecule in SAPO-34_O1 and SAPO-34_O3 as obtained from DFT-D calculations for low water loadings. Selected distances are given in Ångström.

which manifests itself in pronounced differences in the interatomic distances, but not in the interaction energy.

These results can be discussed in the light of some findings from IR spectroscopic experiments: the strongest interaction is calculated for SAPO-34_O1, the system for which the highest ν(OH) stretching frequencies are predicted on the basis of the ν(OH)–d(O–H) correlation. In a real system, in which protons may occupy different sites, the adsorption should preferentially occur at H–O1 at low water loadings. Experimentally, it was observed that the high-frequency band at 3630 cm^{-1} loses intensity more quickly than the low-frequency band at 3600 cm^{-1} when the water loading is gradually increased, which means that the initial adsorption occurs primarily at those protons that contribute to the high-frequency band.[18] There is thus qualitative agreement between the computational predictions and experimental observations, although it has to be reiterated that previous studies ascribed the high-frequency band to different protons than the present work. Based on the preliminary interpretation presented here, future computational work should aim at a comprehensive prediction of the IR spectra in guest-free and water-loaded SAPO-34.

In SAPO-34_Si_island, the interaction of water with the individual protons is 2 to 3 kJ mol^{-1} stronger than in SAPO-34_OX. Table 3 shows that this increase is primarily due to a larger contribution of non-dispersive interactions. There are also systematic differences in the interatomic distances: in particular, the hydrogen bonds between the framework proton and the O_{H_2O} atom are systematically shorter. Together with the slightly increased elongation of the d(O–H) bond when compared to SAPO-34_O1 and _O3, this points to stronger hydrogen bonding. Based on these findings, it can be postulated that protons in the vicinity of the silicon island exhibit a stronger positive polarisation than those near an isolated silicon atom, and thus interact more strongly with adsorbed water molecules. This is in accordance with the previous observation that protons bordering a silicon island exhibit a higher acidity.[14–16]

In the SAPO-34_SiAl_domain system, a more heterogeneous distribution of the individual interaction energies is observed, with values of E_{int} ranging from −86.2 kJ mol^{-1} to −99.1 kJ mol^{-1}. For the cases in which water interacts with H–O1_1 and H–O1_2, the interaction energy and the interatomic distances are relatively similar to those obtained for the corresponding system with isolated Si atoms, SAPO-34_O1. In the system in which water is adsorbed at H–O3, the interaction is nearly 5 kJ mol^{-1} weaker than in SAPO-34_O3, and the elongation of d(O–H) is reduced. This indicates that protons at the border of the aluminosilicate domain are similarly or less positively polarised when compared to those in SAPO-34 with isolated silicon atoms. A different situation is found for water adsorbed at H–O1_3, visualised in Fig. 4: here, the interaction is stronger than in all other cases considered, and a short contact between one of the hydrogen atoms of the water molecule and a framework oxygen atom is formed. As can be seen in Fig. 4, this oxygen atom participates in an Si–O–Al linkage, whereas the secondary H_{H_2O}···O contacts in

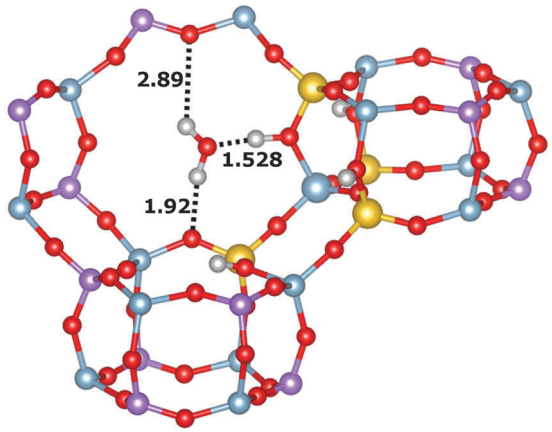

Fig. 4 DFT-D optimised environment of the water molecule in SAPO-34_SiAl_domain, H_2O@H–O1_3. Selected distances are given in Ångström.

all other systems in which water interacts with H–O1 protons (such as the one shown in Fig. 3a) involve framework oxygen atoms that form Al–O–P linkages. Due to the lower electronegativity of silicon in comparison to phosphorus, the shorter $d(H_{H_2O}\cdots O)$ distance and the stronger interaction can straightforwardly be attributed the increased negative polarisation of the framework oxygen atom. Depending on the proton distribution in the aluminosilicate domain (which was not varied in the present study), different local environments in which such favourable interactions occur can be envisaged.

The resulting interaction energies obtained for high water loadings (30 H_2O molecules per unit cell) are summarised in Table 4. Because each of these values was calculated by averaging over five snapshots, the standard deviation is also given (the individual energies for each snapshot, as well as selected plots of final structures, are included in the ESI†). Of the systems with isolated silicon atoms, only SAPO-34_O1 and SAPO-34_O3 were included, since we have seen above that the interaction with water is almost independent of the position of the framework proton. The average interaction energies obtained for the four defect-free SAPO-34 systems considered fall in a rather narrow range (between −69.6 and −70.9 kJ mol^{-1}), which does not extend beyond the typical standard deviation of roughly ±1.5 kJ mol^{-1}. As the interaction strength is practically identical for all systems, there is no evidence that the interaction at high water loadings is significantly affected by variations in the silicon distribution (isolated silicon atoms *vs.* silicon islands or aluminosilicate domains). The interaction is approximately 20 to 25 kJ mol^{-1} weaker than at low loadings, and non-dispersive contributions do not exceed 70% of the total interaction energy (low loadings: ∼78%). This is a consequence of the fact that only few of the adsorbed water molecules can directly interact with the framework protons through relatively strong hydrogen bonds (in some instances forming hydronium ions, see below), whereas the majority of water molecules form weaker hydrogen bonds with framework oxygen atoms and other water molecules. Again, the average interaction energy can be compared to the heat of adsorption: at water coverages above 50 g kg^{-1} (>7 molecules per unit cell) the heat of water adsorption of SAPO-34 lies in the range of 62 to 65 kJ mol^{-1}, and is nearly independent of the loading.[6] The computational predictions are in good agreement with these values.

Table 4 Averaged DFT-D interaction energies (per H_2O molecule) obtained for 30 water molecules per unit cell adsorbed in different models of SAPO-34 and AlPO-34. The average non-dispersive contribution is given in absolute and relative terms

	$E_{int,aver}$/kJ mol^{-1}	$E_{int,nodisp,aver}$/kJ mol^{-1} (%)
SAPO-34_O1	−70.9 ± 2.0	−49.9 (70)
SAPO-34_O3	−70.0 ± 1.6	−48.9 (70)
SAPO-34_Si_island	−70.7 ± 1.3	−49.7 (70)
SAPO-34_SiAl_domain	−69.6 ± 1.2	−48.7 (70)
SAPO-34_defect + $Si(OH)_4$	−70.8 ± 1.4	−47.6 (67)
SAPO-34_desilicated	−67.2 ± 1.7	−44.8 (67)
AlPO-34	−63.5 ± 0.4	−42.0 (66)

Adsorption of water in defect-containing SAPO-34 models

As shown in Fig. 2c, there are four protons associated with the defect in SAPO-34_defect_$Si(OH)_4$ that do not participate in strong hydrogen bonds, and are thus accessible to water molecules. One of these protons is attached to a terminal Al–O–H group associated with the defect (H–Of), and the other three are part of the extra-framework orthosilicic acid group (H–Os1, H–Os2, H–Os3). The interaction energies obtained for water adsorbed at these protons are listed in Table 5. While there is a considerable variation of the interaction energies (from −70.4 to −82.0 kJ mol^{-1}), they are consistently smaller than those obtained for the defect-free SAPO-34 systems. The non-dispersive contribution is also smaller, and the hydrogen bonds are (in most instances) significantly longer. Apparently, the interaction of water with the protons of the $Si(OH)_4$ group or the Al–O–H group is significantly reduced when compared to protons associated with Si–O–Al linkages. While these findings indicate that the sites at which initial adsorption will occur become less favourable due to the introduction of the defect, the average interaction energy obtained for high water loadings (30 H_2O molecules per cell) remains nearly unaffected by the partial desilication: it amounts to −70.8 kJ mol^{-1} (Table 4), and thus falls in the same range as the energies obtained for the defect-free models.

In the completely desilicated model, there is only one framework proton per d6R unit that is accessible to guest molecules (H–Of, see Fig. 2d). The DFT-D calculations predict the interaction with this system to be even weaker than in SAPO-34_defect_$Si(OH)_4$, with E_{int} = −67.1 kJ mol^{-1}. Interestingly, the average interaction energy obtained for 30 H_2O molecules per cell in SAPO-34_desilicated is practically the same as for a loading of 3 molecules per cell, *i.e.* the interaction strength is almost loading-independent. Compared to the defect-free SAPO-34 systems, the interaction at low loadings is weakened by approximately 25 kJ mol^{-1}, while it is reduced by a much smaller, but still significant amount of 3 to 4 kJ mol^{-1} at high water loadings. A graphical summary of the interaction energies obtained for defect-free and defect-containing systems at low and high water loadings is provided in Fig. 5.

It is particularly interesting to compare SAPO-34_desilicated and AlPO-34, as the framework composition of these two

Table 5 DFT-D results obtained for small amounts of water adsorbed in defect-containing models of SAPO-34

	E_{int}/kJ mol^{-1}	$E_{int,nodisp}$/kJ mol^{-1} (%)	d(H···O$_{H_2O}$)/Å	d(H$_{H_2O}$···O)/Å
SAPO-34_defect + Si(OH)$_4$, H$_2$O@H–Of	−74.9	−51.2 (68)	1.693	2.12; 2.31
SAPO-34_defect + Si(OH)$_4$, H$_2$O@H–Os1	−70.4	−50.4 (72)	1.715	2.34; 2.70
SAPO-34_defect + Si(OH)$_4$, H$_2$O@H–Os2	−82.0	−61.4 (75)	1.673	1.90; 2.81
SAPO-34_defect + Si(OH)$_4$, H$_2$O@H–Os3	−77.7	−52.0 (67)	1.533	1.95; 2.05
SAPO-34_desilicated, H$_2$O@H–Of	−67.1	−47.8 (71)	1.705	2.21; 2.64

systems is identical, with the exception of the defect in the former system, where one T atom per d6R unit is replaced by three hydroxyl groups and one aqua ligand. For a loading of 30 H_2O molecules per unit cell, the interaction energy obtained for AlPO-34 amounts to −63.5 kJ mol^{-1}. Thus, the interaction is predicted to be approximately 3.5 kJ mol^{-1} weaker than in SAPO-34_desilicated. The difference arises primarily from a reduced contribution of non-dispersive interactions (Table 4). This observation is in line with the more heterogeneous charge distribution in the vicinity of the defect in the desilicated SAPO-34 model. Finally, it is worth noting that the interaction energy computed for AlPO-34 is in reasonable agreement with the experimental heat of water adsorption measured for the chabazite-type AlPO-Tric (triclinic distortion of AlPO-34), which amounts to 53.6 kJ mol^{-1}.[4]

Structure and bonding of adsorbed molecules at high water loadings

As discussed in the introduction, the possibility of a deprotonation of the framework upon water adsorption has been the topic of numerous experimental and computational studies.[18,25–29] According to a recent periodic DFT investigation, the presence of several water molecules is necessary to stabilise protonated clusters in the pores of aluminosilicate zeolites, with the protonated tetramer $(H_2O)_3{\cdot}(H_3O)^+$ being the smallest stable species at temperatures near room temperature.[29] In order to evaluate whether framework deprotonation is predicted to occur in SAPO-34 at high water loadings, the DFT-D optimised snapshots used to calculate the average interaction energy at a loading of 30 H_2O molecules per cell were analysed in more detail.

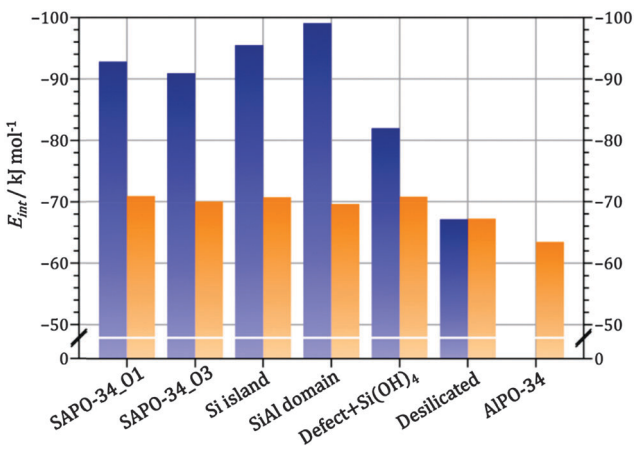

Fig. 5 Comparison of DFT-D interaction energies for different models of SAPO-34. For each system, the blue bar corresponds to the interaction energy obtained for the most favourable adsorption site at low water loadings, whereas the orange bar represents the average interaction energy at a loading of 30 H_2O molecules per unit cell.

In the defect-free systems, a framework deprotonation involving some, but not all framework protons is the most frequently observed situation. Most typically, one or two protons per unit cell are removed from their initial position, forming positively charged $(H_3O)^+$ species. These species sometimes appear in the direct vicinity of the oxygen atom to which the proton was originally attached, but there are also cases where they are located in a completely different region of the pore. A representative example for the former situation is shown in Fig. 6a. In all cases, the H–O bonds of the hydronium ion vary between 1.0 and 1.1 Å, whereas the hydrogen bonds between neighbouring water molecules cover a range from 1.4 to more than 2.0 Å. This range agrees well with the extent of the corresponding maximum in the O–H radial distribution function of liquid water as obtained from experiments and first-principles calculations.[48–50]

In the defect-containing systems, the protons of the hydroxyl groups associated with the framework defect or the extra-framework Si(OH)$_4$ group do not relocate to form positively charged hydronium ions, as this would lead to strongly undercoordinated oxygen atoms. However, the orientation of the hydroxyl groups varies in different snapshots due to the formation of new hydrogen bonds to adsorbed water molecules. On the other hand, one of the protons of the aqua ligand may transfer to an adsorbed water molecule, leading to the formation of a hydronium ion and a defect surrounded by four hydroxyl groups (instead of three OH groups and one aqua ligand). In one rather peculiar case, a proton is shared between two hydroxyl groups, with two short O–H bonds (with a length of 1.166 Å and 1.246 Å respectively), thereby forming a bihydroxide ($H_3O_2^-$) bridge between two aluminium atoms (Fig. 6b).[51–53]

MAS NMR studies on SAPO-34 have shown that water molecules coordinate to framework aluminium atoms at high water loadings, leading to the formation of octahedrally coordinated Al atoms.[19] Similar phenomena have been observed in DFT-based MD studies of water-containing aluminophosphates, such as fully hydrated AlPO-34 and AlPO-18.[54,55] An inspection of the snapshots obtained at a loading of 30 H_2O molecules per cell reveals that five-coordinated aluminium atoms appear in some, but not all of the DFT-D optimised structures. A representative example, taken from one of the snapshots obtained for SAPO-34_O3, is shown in Fig. 7. The coordination environment of the Al atom corresponds to a (more or less distorted) trigonal bipyramid, with the water molecule in one of the axial positions. Characteristically, the distance from the aluminium atom to the axial oxygen atom of the coordinated H_2O molecule ranges between 1.9 and 2.1 Å, and the other axial Al–O bond is elongated with respect to the

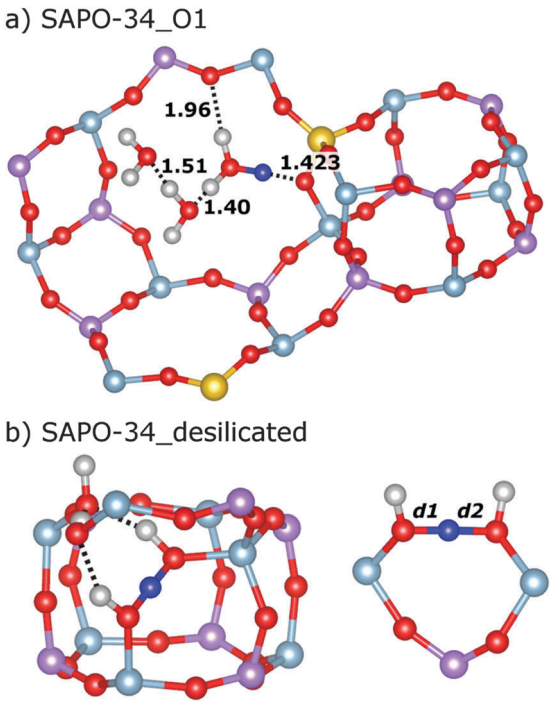

Fig. 6 (a) Representative example of framework deprotonation in SAPO-34_O1. The proton that has relocated from the framework to form a hydronium ion is highlighted in blue. Only the two nearest water molecules are included, and hydrogen bond distances are given in Ångström. (b) Visualisation of bihydroxide anion formation observed in SAPO-34_desilicated. The proton at the centre of the $H_3O_2^-$ anion is shown in blue, and surrounding water molecules are omitted for clarity. The figure on the right hand side shows the direct environment of the bihydroxide anion: d1 = 1.166 Å, d2 = 1.246 Å.

typical bond length of ~1.75 Å observed for tetrahedrally coordinated Al. Among the defect-free systems, formation of five-coordinated Al atoms is found in SAPO-34_O1 and SAPO-34_O3, but not in SAPO-34_Si_island and SAPO-34_SiAl_domain. Since only five snapshots per system were considered, this observation does not allow for definitive conclusions whether a direct coordination of water to framework Al atoms is more likely in systems with isolated Si atoms. Nevertheless, it is worth highlighting that an increased likelihood of the formation of five-coordinated Al in the SAPO-34 models with isolated Si atoms could be linked to the lower hydrolysis stability of these systems: a recent DFT study of the desilication of SAPO-34 by Fjermestad *et al.* indicates that the most likely desilication pathway begins with the formation of five-coordinated aluminium.[23] Because this scenario is energetically less favourable than hydrogen bonding of water to a framework proton, it was concluded that the coordination of isolated water molecules to framework Al atoms can only occur at high temperatures. However, it was also shown that additional water molecules adsorbed in the vicinity may stabilise H_2O–Al bonds. While the importance of such cooperative effects cannot be quantified on the basis of the present results, the calculations indicate that the formation of five-coordinated Al is possible at high water loadings, even when temperature effects are not considered. Regarding the defect-containing SAPO-34 models, five-coordinated

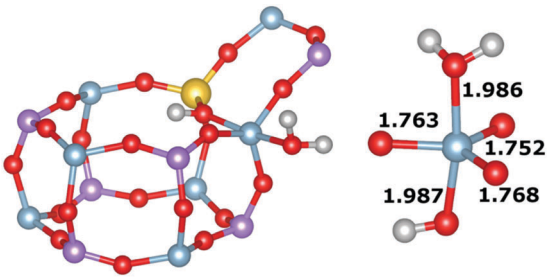

Fig. 7 Formation of five-coordinated aluminium in SAPO-34_O3. Surrounding water molecules are omitted for clarity. The Al–O bond lengths in the AlO_5 coordination polyhedron are shown on the right-hand side (in Å).

aluminium is found in several of the DFT-D optimised snapshots. Both coordination of water molecules to Al atoms associated with the defect, and to Al atoms located in intact regions of the framework occur. In AlPO-34, one case of five-coordinated Al is observed among the five snapshots.

As a final remark to this section, it has to be considered that static structure optimisations were performed in the present work. This approach has inherent limitations: on the one hand, the effect of temperature on the interaction strength cannot be quantified directly, so only estimations are possible. On the other hand, the methodology does not account for temperature-induced distortions of the framework, which might lead to the creation of new adsorption sites. For example, as water molecules at the interior of the d6R unit of AlPO-34 have been observed in a previous study,[54] it would be of particular interest to elucidate to what extent water molecules can diffuse in and out of the d6R units, and whether the accessibility of these regions is different in AlPO-34 and SAPO-34. Despite these limitations, important phenomena occurring at high water loadings, such as the partial deprotonation of the framework and pronounced changes in the coordination environment of the framework aluminium atoms could be observed in the DFT-D optimised structures. In order to study these aspects in more detail, and to include the contribution of temperature effects, it would be necessary to perform *ab initio* MD calculations. Important steps in this direction have been made very recently: a DFT-based MD investigation by De Wispelaere *et al.* has addressed the behaviour of water and methanol in the pores of SAPO-34.[56] Based on the calculations, the authors showed that framework deprotonation occurs upon adsorption, and that the deprotonation is a highly dynamical phenomenon, *i.e.* that the catalytically active sites are very mobile. Furthermore, they investigated the changes of the equilibrium unit cell volume as a function of the loading of guest molecules, and found evidence for volume changes on the order of a few per cent at a temperature of 350 °C.

Conclusions

The DFT-D calculations performed in this study have delivered atomic-level insights into the adsorption of water in defect-free and defect-containing models of SAPO-34, which can be summarised as follows:

1. While a location of the framework proton at the oxygen atom O1 is the energetically most favourable situation in SAPO-34

with isolated silicon atoms, the protons may occupy different positions at finite temperature due to the small difference in energy. In systems with isolated silicon atoms, the interaction with water at both low and high loadings is practically independent of the location of the proton, and the DFT-D interaction energies agree well with heats of water adsorption determined experimentally. In qualitative correspondence with findings from IR spectroscopy, two different binding modes could be identified for low coverages, which depend on the location of the framework proton.

2. Local heterogeneities in the silicon distribution (silicon islands, aluminosilicate domains) lead to a moderately stronger interaction with water at low loadings due to the creation of particularly favourable adsorption sites. On the other hand, their presence does not affect the interaction strength at higher water loadings. Thus, the onset of water adsorption will occur at slightly lower relative pressures than in systems with isolated silicon atoms, whereas the heat of adsorption at higher loadings should be practically the same. This is in line with the experimental observation of very similar heats of adsorption in two different samples of SAPO-34 synthesised *via* the morpholine route (which favours isolated Si atoms) and the tetraethylammonium hydroxide route (favouring Si islands), respectively.[2] We should note, however, that only small 5-atom domains could be investigated in the present study. It can be expected that the presence of larger, purely siliceous regions will tend to weaken the interaction with water due to the hydrophobicity of these areas.

3. The presence of defects created through partial or full desilication leads to a drastic weakening of the interaction with small amounts of water, and to a modestly reduced interaction at high water loadings. It can be concluded that the impact of defects will be twofold: on the one hand, the present results show that defect-containing system will be less attractive for thermal energy storage due to the weaker host–guest interactions. On the other hand, the formation of isolated defects may constitute a first step towards structural decomposition, *i.e.* loss of crystallinity and porosity. This has been found to be a problem for SAPO-34 samples synthesised *via* the morpholine route, as the water uptake capacity of these samples deteriorates rapidly over a few cycles in adsorption–desorption experiments.[2]

4. At low water loadings, the adsorbed water molecules are bonded exclusively through hydrogen bonds, and there are no indications for framework deprotonation. On the other hand, the DFT-D calculations predict a certain degree of framework deprotonation at high water loadings. While this finding is in agreement with previous computational studies, only smaller amounts of water were considered in these earlier works (at most 4 water molecules per proton, compared to $\sim$10 H_2O molecules per proton in the present work).[27–29] *Ab initio* MD calculations could be employed to quantify the extent of framework deprotonation, and to assess possible differences among systems with isolated Si atoms and local heterogeneities or defects. The same applies for the changes in the coordination environment of framework aluminium atoms upon water adsorption: the static DFT-D calculations used here provide evidence for the formation of five-coordinated Al atoms at high water loadings, but a more detailed evaluation would require an MD approach. In particular, it would be interesting to assess whether five-coordinated Al atoms retain their trigonal-bipyramidal coordination, or whether they constitute an intermediate species that will transform into octahedral coordination through interaction with another water molecule.

There is a body of experimental work pointing to the higher stability of SAPO-34 materials incorporating silicon islands in comparison to systems with isolated Si atoms.[2,3,21] Due to the positive influence of Si islands on the stability, and the absence of a detrimental effect on the water adsorption properties, synthesis routes or post-synthesis treatments that lead to the formation of silicon islands should be favoured when targeting SAPO-34 materials for applications involving water adsorption. While this conclusion had been established already from experiments on a phenomenological basis, the present study has provided microscopic insights into the actual impact of local heterogeneities and defects on the water adsorption properties that could not be obtained experimentally. Future computational work could aim at a more detailed understanding why systems with heterogeneous silicon distributions are more stable than those with isolated silicon atoms, or at a comparison of proton-exchanged and cation-exchanged SAPO-34 systems.

Acknowledgements

I am grateful to Prof. Dr Andreas Lüttge and Dr Rolf Arvidson (Marum, Bremen) for generous access to the Asgard cluster, on which the DFT calculations were run. Dr Alexandra Lieb (Magdeburg University) is acknowledged for enabling the Monte Carlo simulations. The software used for these calculations was funded by the Bundesministerium für Bildung und Forschung (BMBF young researcher group NEOTHERM, grant number 03SF0450). Furthermore, I would like to thank Dr Frank Hoffmann (University of Hamburg) and Dr Rob Bell (University College London) for a critical reading of the manuscript. Funding was provided by the Central Research Development Fund (CRDF) of the University of Bremen (Funding line 04 – Independent Projects for Post-Docs).

References

1 E.-P. Ng and S. Mintova, *Microporous Mesoporous Mater.*, 2008, **114**, 1–26.
2 S. K. Henninger, F. P. Schmidt and H.-M. Henning, *Appl. Therm. Eng.*, 2010, **30**, 1692–1702.
3 S. K. Henninger, G. Munz, K.-F. Ratzsch and P. Schossig, *Renewable Energy*, 2011, **36**, 3043–3049.
4 A. Ristić, N. Z. Logar, S. K. Henninger and V. Kaučič, *Adv. Funct. Mater.*, 2012, **22**, 1952–1957.
5 J. Jänchen, D. Ackermann, E. Weiler, H. Stach and W. Brösicke, *Thermochim. Acta*, 2005, **434**, 37–41.
6 J. Jänchen and H. Stach, *Sol. Energy*, 2014, **104**, 16–18.
7 J. Bauer, R. Herrmann, W. Mittelbach and W. Schwieger, *Int. J. Energy Res.*, 2009, **33**, 1233–1249.

8 S. Shimooka, K. Oshima, H. Hidaka, T. Takewaki, H. Kakiuchi, A. Kodama, M. Kubota and H. Matsuda, *J. Chem. Eng. Jpn.*, 2007, **40**, 1330–1334.
9 G. Sastre, D. W. Lewis and C. R. A. Catlow, *J. Mol. Catal. A: Chem.*, 1997, **119**, 349–356.
10 R. Vomscheid, M. Briend, M. J. Peltre, P. P. Man and D. Barthomeuf, *J. Phys. Chem.*, 1994, **98**, 9614–9618.
11 M. Zokaie, U. Olsbye, K. P. Lillerud and O. Swang, *Microporous Mesoporous Mater.*, 2012, **158**, 175–179.
12 A. Buchholz, W. Wang, M. Xu, A. Arnold and M. Hunger, *Microporous Mesoporous Mater.*, 2002, **56**, 267–278.
13 W. Shen, X. Li, Y. Wei, P. Tian, F. Deng, X. Han and X. Bao, *Microporous Mesoporous Mater.*, 2012, **158**, 19–25.
14 G. Sastre, D. W. Lewis and C. R. A. Catlow, *J. Phys. Chem. B*, 1997, **101**, 5249–5262.
15 G. A. V Martins, G. Berlier, S. Coluccia, H. O. Pastore, G. B. Superti, G. Gatti and L. Marchese, *J. Phys. Chem. C*, 2007, **111**, 330–339.
16 K. Suzuki, T. Nishio, N. Katada, G. Sastre and M. Niwa, *Phys. Chem. Chem. Phys.*, 2011, **13**, 3311–3318.
17 M. Zokaie, U. Olsbye, K. P. Lillerud and O. Swang, *J. Phys. Chem. C*, 2012, **116**, 7255–7259.
18 S. Bordiga, L. Regli, C. Lamberti, A. Zecchina, M. Bjørgen and K. P. Lillerud, *J. Phys. Chem. B*, 2005, **109**, 7724–7732.
19 A. Buchholz, W. Wang, A. Arnold, M. Xu and M. Hunger, *Microporous Mesoporous Mater.*, 2003, **57**, 157–168.
20 C. Minchev, Y. Neinska, V. Valtchev, V. Minkov, T. Tsoncheva, V. Penchev, H. Lechert and M. Hess, *Catal. Lett.*, 1993, **18**, 125–135.
21 M. Briend, R. Vomscheid, M. J. Peltre, P. P. Man and D. Barthomeuf, *J. Phys. Chem.*, 1995, **99**, 8270–8276.
22 T. Fjermestad, S. Svelle and O. Swang, *J. Phys. Chem. C*, 2013, **117**, 13442–13451.
23 T. Fjermestad, S. Svelle and O. Swang, *J. Phys. Chem. C*, 2015, **119**, 2073–2085.
24 T. Fjermestad, S. Svelle and O. Swang, *J. Phys. Chem. C*, 2015, **119**, 2086–2095.
25 L. Marchese, J. Chen, P. A. Wright and J. M. Thomas, *J. Phys. Chem.*, 1993, **97**, 8109–8112.
26 L. Smith, A. K. Cheetham, R. E. Morris, L. Marchese, J. M. Thomas, P. A. Wright and J. Chen, *Science*, 1996, **271**, 799–802.
27 Y. Jeanvoine, J. G. Ángyán, G. Kresse and J. Hafner, *J. Phys. Chem. B*, 1998, **102**, 7307–7310.
28 J. Limtrakul, P. Chuichay and S. Nokbin, *J. Mol. Struct.*, 2001, **560**, 169–177.
29 M. V. Vener, X. Rozanska and J. Sauer, *Phys. Chem. Chem. Phys.*, 2009, **11**, 1702–1712.
30 S. J. Clark, M. D. Segall, C. J. Pickard, P. J. Hasnip, M. I. J. Probert, K. Refson and M. C. Payne, *Z. Kristallogr.*, 2005, **220**, 567–570.
31 J. P. Perdew, K. Burke and M. Ernzerhof, *Phys. Rev. Lett.*, 1996, **77**, 3865–3868.
32 A. Tkatchenko and M. Scheffler, *Phys. Rev. Lett.*, 2009, **102**, 073005.
33 B. Santra, J. Klimes, A. Tkatchenko, D. Alfè, B. Slater, A. Michaelides, R. Car and M. Scheffler, *J. Chem. Phys.*, 2013, **139**, 154702.
34 D. Tunega, T. Bučko and A. Zaoui, *J. Chem. Phys.*, 2012, **137**, 114105.
35 M. Sacchi and S. J. Jenkins, *Phys. Chem. Chem. Phys.*, 2014, **16**, 6101–6107.
36 M. Fischer, *Z. Kristallogr. – Cryst. Mater.*, 2015, **230**, 325–336.
37 M. Amri and R. I. Walton, *Chem. Mater.*, 2009, **21**, 3380–3390.
38 C. Baerlocher and L. B. McCusker, http://www.iza-structure.org/databases/, 2012.
39 F. J. Torres, P. Ugliengo, B. Civalleri, A. Terentyev and C. Pisani, *Int. J. Hydrogen Energy*, 2008, **33**, 746–754.
40 L. Smith, A. K. Cheetham, L. Marchese, J. M. Thomas, P. A. Wright, J. Chen and E. Gianotti, *Catal. Lett.*, 1996, **41**, 13–16.
41 L. Smith, A. Davidson and A. Cheetham, *Catal. Lett.*, 1998, **49**, 143–146.
42 M. Elanany, M. Koyama, M. Kubo, P. Selvam and A. Miyamoto, *Microporous Mesoporous Mater.*, 2004, **71**, 51–56.
43 J.-R. Hill, A. R. Minihan, E. Wimmer and C. J. Adams, *Phys. Chem. Chem. Phys.*, 2000, **2**, 4255–4264.
44 R. Shah, J. D. Gale and M. C. Payne, *Chem. Commun.*, 1997, 131–132.
45 Y. Jeanvoine, J. G. Ángyán, G. Kresse and J. Hafner, *J. Phys. Chem. B*, 1998, **102**, 5573–5580.
46 R. Shah, J. Gale and M. Payne, *Phase Transitions*, 1997, **61**, 67–81.
47 P. Nachtigall, O. Bludský, L. Grajciar, D. Nachtigallová, M. R. Delgado and C. O. Areán, *Phys. Chem. Chem. Phys.*, 2009, **11**, 791–802.
48 A. K. Soper, *Chem. Phys.*, 2000, **258**, 121–137.
49 Z. Ma, Y. Zhang and M. E. Tuckerman, *J. Chem. Phys.*, 2012, **137**, 044506.
50 M. Del Ben, M. Schönherr, J. Hutter and J. VandeVondele, *J. Phys. Chem. Lett.*, 2013, **4**, 3753–3759.
51 K. Abu-Dari, K. N. Raymond and D. P. Freyberg, *J. Am. Chem. Soc.*, 1979, **101**, 3688–3689.
52 C. McMichael Rohlfing, L. C. Allen, C. M. Cook and H. B. Schlegel, *J. Chem. Phys.*, 1983, **78**, 2498–2503.
53 G. De Munno, D. Viterbo, A. Caneschi, F. Lloret and M. Julve, *Inorg. Chem.*, 1994, **33**, 1585–1586.
54 G. Poulet, P. Sautet and A. Tuel, *J. Phys. Chem. B*, 2002, **106**, 8599–8608.
55 G. Poulet, A. Tuel and P. Sautet, *J. Phys. Chem. B*, 2005, **109**, 22939–22946.
56 K. De Wispelaere, B. Ensing, A. Ghysels, E. J. Meijer and V. Van Speybroeck, *Chem. – Eur. J.*, 2015, **21**, 9385–9396.
57 K. Momma and F. Izumi, *J. Appl. Crystallogr.*, 2011, **44**, 1272–1276.